

Interactive comment on “Using computational fluid dynamics and field experiments to improve vehicle-based wind measurements for environmental monitoring” by Tara Hanlon and David Risk

Tara Hanlon and David Risk

thanlon@stfx.ca

Received and published: 25 April 2019

We would like to thank Anonymous Reviewer #1 for their time in suggesting changes that will improve our manuscript. Our responses to the review comments are provided below.

Summary: The experiment, as suggested by the abstract, is well motivated and designed. The abstract is exceptionally well written. However, the paper does not meet the expectations from the abstract. I believe that major changes can make this work

Printer-friendly version

Discussion paper



an extremely useful contribution. Critical details regarding calculations are missing. The CFD work appears to be well done, except for one very worrisome statement that I suspect the authors can easily explain. However, the CFD work is not useful as presented because it is not put in the context of a moving car, as could be done if the above mentioned equations were added to the paper. The bias adjustments presented in the field study appear to be an artifact of experimental design, rather than physically meaningful. This is again because the above mentioned equations were not used. The promise of meaningful use of the stationary anemometers was not fulfilled. These could have been used to make a correct assessment of biases as a function of the speed of the car (using the above mentioned equations), but this work was not done. While the authors are to be commended on obtaining useful observations and CFD calculations, they should redo the non-CFD work and present the final results in a context that combines the conclusions from the CFD results and field results. Such a reanalysis would make an extremely useful contribution. Furthermore, the field data are not made publicly available, which is preferred and often a requirement for modern journal publications.

We appreciate this summary and have used the comments to make changes as suggested in the detailed comments, where the reviewer expands on these general comments.

Major Comments:

1) Section 2.1, end of first paragraph. Please say why these two sets of experiments of experiments appropriate to address the research objectives. I agree that they are appropriate, but some readers will not understand how they can be combined. This point is not addressed in the conclusions either, making this work needlessly incomplete. The relevant equations are presented in a variety of ways in:

Smith, R. S, M. A. Bourassa, and R. J. Sharp, 1999: Establishing more truth in true winds. *J. Atmos. Oceanic Technol.*, 16, 939-952.

[Printer-friendly version](#)[Discussion paper](#)

We have added the following text at to P3 L9 in section 2.1:

“By evaluating the vehicle’s external flow field under both varying vehicle speed and wind yaw angle we can quantify the bias the vehicle shape induces on a truck mounted anemometer and calibrate the measurements prior to correcting wind speed and direction measurements for the vehicle’s motion.”

The following text has been added into the Results and Discussion section on P10 L6:

“The empirical calibration must be applied to remove the bias of the vehicle’s shape on anemometer measurements prior to correcting for the vehicle motion.”

The above reference has also been used to address minor comment 3 and add further description to the field methods.

Page 4: lines 10 and 11: The meaning of ‘The drag coefficient was determined when the change in CD was less than 0.001.’ is not clear. Is this condition sufficient? Or is convergence slow enough that this condition leads to large errors. How was it determined that this condition is sufficient, as 0.001 is rather a large fraction of the drag coefficient over a smooth surface? The following sentences are insufficient for such a test. Granted, this situation becomes clear later, but it should be clear when presented.

We wanted the CFD results to match the instrument accuracy available in our field tests. As our model was simplified, we knew we could not expect perfect accuracy in the drag coefficient. 0.001 is less than 1% of the manufacturers reported drag coefficient (0.386), and less than the instrument errors used in the collection of field measurements.

3) Separating the experimental design (for two experiments) from the results (for two experiments) is irritating and needlessly confusing. After the experimental design for the CFD I would greatly prefer to see the results from the CFD. a. Why are limitations of the CFD method/results discussed in the section on field observations? b. If this lack of results from flow into the wind is true (as literally read), then why should I read

[Printer-friendly version](#)

[Discussion paper](#)



further? This seems like it could be critical flaw.

We have restructured the manuscript to address this point. We have inserted a discussion section at P14 L7. In this section we discuss the results together, and the limitations from CFD are discussed in this section and no longer in the field results.

4) Are the observational data made publicly available? If so where? If not, should this work be published?

Field data have been made available at: https://figshare.com/articles/Mobile_and_Stationary_Anemometer_Wind-SoutheasternSK_May2017_csv/8035235,

doi = "10.6084/m9.figshare.8035235.v1"

5) Page 10, Equation 1 and following line: What are the units of wind direction and wind speed? There will be quite a difference for m/s vs mph, and for radians vs. degrees!

We have modified presentation of the equation to be more descriptive with assigned variables and include units. The equation was modified to include both the anemometer windspeed (AWS,) and the corrected windspeed (WS) for clarity.

The following text has been added to P10 L1 :

“The polynomial pictured in Fig 5 is multiplied by the Anemometer windspeed (AWS), to give the corrected wind speed (WS). Equation 2 gives the side-mounted anemometer’s correction function for wind direction (WD) measurements ranging from $-40^\circ < WD < 40^\circ$. Wind speed units are in km h^{-1} and wind direction units are in degrees.

6) Figure 6: It appears that there are fluctuations in the ratio of anemometer wind speed to vehicle wind speed that is associated with the speed of the car. This is not surprising because the measured speed is equal to the magnitude of ‘the wind velocity minus the car velocity.’ Such a dependency is expected as an artifact of the situation, and not as a systematic correction in the manner that the authors suggest. Showing the math requested in comment (1) would help the authors organize their thoughts and

Printer-friendly version

Discussion paper



experiment in a manner that conveys useful information. I had expected the authors to use differences from the stationary anemometers to illustrate these biases, but that work is not contained in this paper.

The objective of this figure is to show that the short anemometer placement consistently measures higher wind speeds than the tall anemometer placement. The manuscript has been edited to better describe the figure and its importance of anemometer height a top the vehicle.

The statement , “Figure 6 shows the tall and short anemometer measurements scaled with vehicle speed” has been modified to say “Figure 6 shows magnitude of the tall and short anemometer measurements when normalized by the vehicle speed.”

The reference to Smith et al., 2009 from comment 1 has been used to add an equation and text to P7 L4. Please refer to our response to minor comment 3 and detailed comment 9 in our Response to RC2 for the detailed changes.

7) Page 12, figure 8: What is actually shown in Fig. 8b? The caption and text claim that the figure shows the corrections, which suggests that the corrections are nearly identical to the measured winds. It appears that what is shown is the corrected winds.

Please refer to our Response to RC2 for revisions proposed for Fig. 8.

Minor Comments: 1) Line 3: ‘Used to study Meteorology’ is too broad. Be more specific about the scale and the type of vehicle (for example, ships are vehicles, but not included in this study).

The text has been replaced to say, “Currently, land vehicle-based wind measurements are used to study severe weather-related mesoscale meteorology (Belusic et al., 2014, Straka et al., 1996), lake meteorology (Taylor et al. 2011; Curry et al. 2017) and are integrated into methane measurement studies to detect, quantify, and map emission plumes from oil and gas developments (Atherton et al., 2017; et al., 2015; Zazzeri et al., 2015).

[Printer-friendly version](#)[Discussion paper](#)

2) Table 1: Improve the caption to explain the labels of the table rows and columns.

The caption has been changed to “Drag comparison of three turbulence models with inlet velocity of 22.2 m/s. The drag coefficient (CD) for each turbulence model is reported with the number of iterations required to achieve a solution and the percent difference (ΔCD) from the manufacturers reported CD of the vehicle model.”

The turbulence models in the rows of the table are described on P4 L7 before introducing the table.

3) Page 6, line7 and line 10-12: How were these corrections made? Was the car motion subtracted from the wind, or was the adjustment done correctly following Smith et al. 1999)? The statement that the calculations were done is R does not tell us how they were done. Smith, R. S, M. A. Bourassa, and R. J. Sharp, 1999: Establishing more truth in true winds. J. Atmos. Oceanic Technol., 16, 939-952. How was the temporal averaging done? See the above paper for the importance of the correct averaging while wind directions are changing relative to the vehicle.

We have added the following text to P6 L7:

“To correctly compute true winds, vehicle based wind must be corrected for the vehicle’s motion over the fixed earth. The vehicle vector has a direction equivalent to the vehicle’s course over the ground, and a magnitude equivalent to the vehicle’s speed over the ground (Smith et al., 1999).”

Please also refer to detailed comment #9 our Response to RC2, where we describe the subtraction equation.

The averaged vehicle-based anemometer measurements presented in Figure 8 were calculated by expressing all of the wind speed and direction measurements in complex exponential form to keep wind speed and direction as one vector, as opposed to separating them into components. Figure S1 in the supplement details how the components of each vector were calculated, and how the averaging was done.

[Printer-friendly version](#)[Discussion paper](#)

4) Page 7, line 3: ‘similar qualitative trends’ is so vague as to be nearly meaningless.

P7 L3 has been modified to say, “The CFD and field experiments showed that the measured wind at the anemometer location varied under wind yaw angle. The bias found in the CFD varied with the rotation of the truck, and the field results concluded that the measured wind differed in head, cross and tail wind conditions.”

5) Page 7, line 10: This statement makes sense only for a fixed wind speed and direction. If it is being applied in general as suggested by the writing, then this result cannot be correct – or important caveats are missing.

P7 L10 has been modified to:

“In each computational domain, we found that the wind bias scaled with vehicle speed and the amount of bias (slope) differed with the location above the vehicle.”

6) Page 7, lines 21-22 & page 8, line 3 The logic ‘(where measured windspeed = true windspeed)’ must be missing key caveats.

The following text on P7 L21: “ This observation is similar to a conclusion by Moat et al. (2005), stating that shipboard anemometers should not be placed close to the line of equality (where measured wind speed = true wind speed) as high pressure gradients are present in this region. The line of equality would be expected to move vertically to some degree, according to the ground and/or wind speed.”

References the work Moat et al., conducted on airflow distortion at anemometer sites on ships. As part of the study, the authors used Vectis CFD code to model the flow over generic voluntary observing ship models. The study presents the flow pattern above a bulk carrier model, and shows that above the bridge there exists a decelerated region of flow and at a greater height above the bridge, an accelerated region of flow. Between the decelerated region and accelerated region of flow there exists a line where the flow is equivalent to the wind speed. In this region the velocity gradients are very steep, and sensitive to bias. Moat et al., concluded that an anemometer should not be placed in

[Printer-friendly version](#)[Discussion paper](#)

this region.

In our CFD model, we also found that a decelerated region of flow existed below the accelerated region of flow. We recommend placing the anemometer above this region to avoid the steep velocity gradients, and referenced this text to support our results.

7) Page 7, line 34: 'How big is 'significant' in terms of heights? The existing text is too vague.

P 7 L 34 has been replaced with "When exposed to large yaw angles, the wind bias over the truck at low heights can be twenty percent, and even at a height of 1.7 m above the vehicle, a bias of greater than 5 percent is present."

8) What is meant by wind speed > 3 standard deviations? Standard deviations of what (relatively to what)?

Good point. This information was lacking in the manuscript. The yellow circles represent wind speed measurements that are greater than 3 standard deviations away from the mean wind speed measurement. The mean wind speed measurement is calculated specific to a) the wind speed measurements from the vehicle-based anemometer after the frontal-correction was applied, b) the wind speed measurements from the vehicle-based anemometer after the empirical correction, and then frontal correction was applied, c) the wind speed measurements from the stationary anemometer located at the 4 different vehicle bearings.

The caption of Figure 7 has been modified to include: " The yellow circles represent wind speed measurements that are greater than three standard deviations away from the mean wind speed of the wind speed measurements calculated with the a) frontal correction applied, b) empirical correction and frontal correction applied, and c) specific to the stationary anemometer at each bearing."

9) Page 9, line 2: What is meant by 'normalized wind speed'?

The normalized wind speed is the measured wind speed divided by the inlet velocity.

Printer-friendly version

Discussion paper



The text has been changed to:

“The normalized wind speed (measured wind speed: inlet speed) at the location of an anemometer mounted in the same location as the field test was computed for each yaw angle simulation.”

10) Page 10: At or near the end of the CFD results, please remind the reader that these are CFD results rather than field results. Changing the order of the paper to put method and results together would reduce this problem. a. The last line of this section belongs in the section on field results b. How was this yaw determined? c. How was temporal averaging applied? Was it after individual calculations were corrected, or was the averaged corrected? The first approach is correct when the vehicle relative wind direction is changing.

a) This has been addressed with by the addition of a discussion section in response to major comment 3. b) The yaw is determined by the raw anemometer wind direction measurements. c) There is no temporal averaging on the mobile measurements.

Please also note the supplement to this comment:

<https://www.atmos-meas-tech-discuss.net/amt-2018-354/amt-2018-354-AC2-supplement.pdf>

Interactive comment on Atmos. Meas. Tech. Discuss., doi:10.5194/amt-2018-354, 2018.

Printer-friendly version

Discussion paper



Interactive comment on “Using computational fluid dynamics and field experiments to improve vehicle-based wind measurements for environmental monitoring” by Tara Hanlon and David Risk

Tara Hanlon and David Risk

thanlon@stfx.ca

Received and published: 25 April 2019

We would like to thank Anonymous Reviewer #2 for their time in suggesting changes that will improve our manuscript. Our responses to the review comments are provided below in blue.

General Comments:

The reasons for focusing on installation of an instrument atop of a pickup cap are not provided and not clear. Much of the initial discussion focuses on the work of Straka et

Printer-friendly version

Discussion paper



al. (1996) and others that chose to put the anemometer out front of the vehicle to avoid the vehicle's flow field. And the authors show in their results (e.g. Fig. 3) that such a location would indeed be preferable. The authors need to be much more clear about the reasons to choosing to focus only on one location on top of a cap.

Problems with wind direction and speed data from a mobile instrument occur when the vehicle is experiencing acceleration (either changes in speed or direction). Data under such conditions should be removed from the analysis. However this issue is not mentioned by the authors, even though it has a significant influence on both methods and results. I can only assume the authors have left these data in, and it helps to explain some of the large scatter in Fig. 7. This issue needs to be fully addressed.

The authors provide corrected wind data in Figs. 7 and 8 but readers (including myself) will want to see uncorrected data in these plots as well. This will have the side benefit of making the plots larger and more legible.

Lastly, there is quite a bit of material relating to ships in the paper, and the reason is not entirely clear. Unless the authors can justify the inclusion of all of this material, it would be good to pare this down to essentials.

We appreciate these general comments. We have used these general remarks to direct each detailed change suggested in comments below.

Detailed Comments

1. Page 2 Line 3 – There have been a number of other field studies that have made use of mobile measurements, including studies in Canada related to severe weather-related mesoscale meteorology (Taylor et al. 2011, Curry et al. 2017), air quality (Brook et al. 2013) and urban meteorology (Joe et al. 2018). The authors should consider including these in the literature review and possibly make use of some of the results.

We have considered the recommended literature, and updated the manuscript with the following:

A reference to Curry et al., 2017 and Taylor et al., 2011 has been added to Page 2 Line 3 of the manuscript.

We have used the literature to add to the discussion in the manuscript. We comment on the updates in detailed comments 25 and 26.

2. P4 L10 – re 22.222 m/s – do the authors believe the inlet velocity could be controlled to this accuracy? Please use a reasonable number of significant digits.

The text has been modified, 22.222 m/s has been replaced with 22.2 m/s.

3. P4 L26 - To eliminate confusion here, it should read "The flow around a pickup truck with an open box is more complex than...because of wake interactions".

P4 L26 has been modified to "The flow field around a pickup truck is more complex than the flow around an SUV of sedan because of wake flow interactions."

4. P4 L31 – Why is this the 'area of interest', and what evidence is there to support that flow atop the cap of the vehicle is located away from large pressure gradients?

The text "Our area of interest, the flow atop the cap of the vehicle is located away from large pressure gradients. Because the cap eliminates large pressure gradients at the area of interest, $k-\epsilon$ performance in the drag comparison, and its results in other studies, we have selected the $k-\epsilon$ turbulence model as appropriate for our analysis in the velocity field above a capped pickup truck."

Has been replaced with,

"Our motivation for placing an anemometer atop a pick-up truck came to assist vehicle-based gas monitoring systems (Atherton et al., 2017; Baillie et al., 2019; O'Connell et al., 2019) measuring gas emissions to achieve practical placement and further calibration practices. In these studies, the anemometer was mounted above a truck cap. Because of the differing vehicle shape from an open bed pickup truck, $k-\epsilon$ performance in the drag comparison, and performance in other studies, we have selected the $k-\epsilon$

[Printer-friendly version](#)[Discussion paper](#)

turbulence model as appropriate for our analysis in the velocity field above a capped pickup truck.”

We removed the statement , “Because the cap eliminates large pressure gradients at the area of interest” in the methods portion of the manuscript, as we have not yet presented our CFD results.

5. P5 L5 - Were the speeds ranging from 40 to 100 also applied to these eight domains? Need to be more clear about this.

Yes, the same speed ranges were applied to all eight domains. The following text has been added to P5 L10:

“We used the additional computational domains to test all combinations of yaw under inlet speeds ranging from 40 km h⁻¹ to 100 km h⁻¹ in 5 km h⁻¹ increments.

6. P5 L16 – Given known problems with measuring during acceleration, why make fixed measurements in the corners rather than the straight-aways? Why were the corners chosen in the first place?

The following text has been added to P5 L17:

“The stationary anemometers were placed on the corners to provide opportunity for comparison with both legs of the straightaway. This ensured that we would have data for comparison with each leg should an anemometer malfunction.

We consistently found locations with flat, treeless terrain and no surrounding infrastructure at locations approximately 300 m from each corner. The accessibility of these stationary anemometer sites also influenced our selection of placing the stationary anemometers near the corners.

7. P5 L19 – The meaning of this sentence is not clear – what is the ‘frontal wind’ from the vehicle? Please revise.

This sentence was unclear and not necessary, it has been removed.

[Printer-friendly version](#)[Discussion paper](#)

8. P6 L1 – Data should only be used when the vehicle speeds were kept constant – the authors do not mention this, and should fully explain their decisions here.

This is an excellent point. The objective of our field study was to collect measurements at fixed vehicle speeds that could be compared with stationary anemometers. The measurements from the corners when the vehicle was turning, and accelerating up to cruise control speed should be excluded. The following text has been inserted to P6 L6:

“The 1Hz geolocation measurements were used to compute the vehicle speed and bearing, field measurements that deviated more than 2.5 km h⁻¹ from the implemented cruise control speed, vehicle bearing measurements that differed more than 5° from designated vehicle course were removed from the data set.”

Figure 7 and 8 have been modified to exclude non-steady-state measurements.

9. P6 L12 – I would like to see the detailed calculations included in an appendix.

We removed the text, “and a true wind vector was computed by removing the vehicle vector from the vehicle wind vector. All computations were completed using R 3.4.1 statistical software (R Core Team. 2016)”

And replaced it with, “We calculated the vehicle’s course over the ground using the GPS coordinates to obtain a vector of equal magnitude and opposite direction to be the frontal wind induced by the vehicle’s motion (F). We compute the meteorological wind vector (W) by subtracting the frontal wind induced by the vehicle’s motion (F) from the raw anemometer measured wind vector (A). The calculation is presented in Equation (1) . The computation comes from the method calculating the meteorological true wind from a moving vessel presented by Smith et al., 2009.

$$W = A - F$$

We have included a figure and details describing the vector translation required in the computation to S1 in the supplementary information.

[Printer-friendly version](#)[Discussion paper](#)

10. P7 L25 – The meaning of this sentence is not clear to me. Please reword.

P7 L25 has been reworded to say “The second set of simulations in this study are of particular interest because they evaluate the flow field under cross wind conditions. Many previous CFD and wind tunnel studies (Yang and Khalighi 2009; Holloway et al., 2009) examine the flow field resulting from inlets, which direct the airflow along the longitudinal axis of the vehicle. Aside from Houston et al. 2016, we have not found studies using CFD to conduct crosswind experiments to study the flow field around a vehicle.

11. P8 L14 – It is not clear what these sentences are referring to – I see nothing in Table 2 that “shows” this.

The two sentences beginning on P8 L14 have been reworded to say:

“Table 2 shows that the height required for an anemometer to experience bias below 2% increases with increasing yaw angle. Anemometer heights selected through frontal wind tunnel tests would still experience bias under cross wind conditions.”

12. Figure 7 – A few problems here – the grey bars need to be explained, another panel that shows the uncorrected mobile measurements needs to be included, and the separation of data at 0/360 degrees needs to be addressed so that there are only four ‘bars’ of C3 data, as in the control.

The following changes have been made to figure 7 to address both the above detailed comment and the general comments made by the reviewer.

The measurements have been regrouped so that the figure shows measurements corresponding to vehicle bearing measurements of 0°, 90°, 180°, 270° corresponding to the vehicle travelling in the North, East, South and West directions. This change removes the separation of the data at 0° and 360°.

The grey bars represent measurements that were collected in tail wind conditions. A second sentence has been added to the figure caption that reads, “The shaded

grey bars represent measurements acquired when the vehicle was driving in tail wind conditions.”

The change addressed in detailed comment 8 reduces the scatter in this figure. Figure 7 now includes measurements where the vehicle speed deviates no more than 2.5 km h⁻¹ from the implemented cruise control speed, and the vehicle bearing measurements differ no more than 5° from designated vehicle course.

13. Page 11 L5 – ‘data was’ should be ‘data were’

This change has been made

14. Figure 8 – A few issues here – the wind rose plot details are illegible particularly the frequency values (which appear to be missing entirely), a diagram the uncorrected mobile winds needs to be included, and the reason needs to be given to explain the WNW winds measured only along the top, headwind leg. The authors also need to specify what samples are being plotted here – certainly not 1 Hz data.

The following changes have been made to figure 8:

The measurements presented in the figure have been modified to reflect the change made in response to detailed comment 8, removing measurements outside of the speed test. The data was previously the 70 km h⁻¹ speed test, but was replaced with the 60 km h⁻¹ speed test because fewer measurements were excluded as a result of being 2.5 km h⁻¹ outside the speed test range.

The wind rose frequency values are now legible. The stationary anemometers report one minute averages. The instrument collects a wind speed and direction measurement every 10 seconds and reports the average of those six. The instrument also reports a wind gust measurement which is the highest instantaneous wind speed measured during the selected averaging interval. The wind roses are the average wind direction measurement and wind gust reported for each minute. The wind roses contain 14 minutes of data, and are the measurements acquired during the 60 km h⁻¹

[Printer-friendly version](#)

[Discussion paper](#)



speed test.

Adding another plot with raw measurements to Figure 8 is not ideal for space, this plot is added to appendix A.

15. P12 L7 – The use of ‘levels’ as a verb here is confusing. Please reword.

P12 L7 has been reworded to say, “Applying the empirical correction reduces the difference in the mean of the wind direction measurements across the four vehicle bearings.”

16. P13 L4 – Over what periods are the data for the wind roses taken? This needs to be specified.

The data displayed in the wind roses was taken over a 14 minute period, which was the duration of the 60 km h⁻¹ field test. This information has been added to the manuscript to further describe 8.

The following text has been added to P13 L4, “ The measurements in the wind roses are the wind gust and average wind direction measurements reported each minute of the 14 minute time speed test.”

17. P13 L5 – Why not also average the winds over the leg and compare to the wind rose over that leg?

Figure 8 has been modified to include a table comparing the mobile measurements averaged over the leg with the average from the wind rose.

The wind rose at each corner is a representation of the wind patterns we would expect to see across the survey leg. We did not obtain raw one second measurements from the stationary anemometers making it difficult to average the measurements in an identical way. Our study instead uses the stationary measurements as a guide to evaluate the accuracy and precision of the 1 Hz vehicle-based anemometer measurements.

18. P13 L10 – The authors drove the route at speeds of 40, 50, 60, 70, and 80 km/h but only present results from 70 km/h in Fig 8. They need to also show results from the

[Printer-friendly version](#)[Discussion paper](#)

other speeds (perhaps best using averages).

Figure 8 was constructed to show – in detail - the variability in the mobile wind measurements after the CFD calibration was applied. It was more the purpose of Figure 7 to show the general impact of the CFD calibration across all speed tests.

19. P13 L10 – Re “improved”, it is difficult to see this and is not quantitative. The authors need to better support/interpret the results.

The text “Figures 7 and 8 demonstrate that measurement reliability and likely accuracy is improved by applying an empirical correction to vehicle anemometer measurements prior to correcting for the vehicle vector. The empirical correction from CFD improved the field measurements, but still could improve in tail wind.”

Has been changed to “Figure 8 shows that applying the CFD calibration improves the agreement of the average mobile wind speed and direction measurements with the average stationary measurements in three of the four legs of the route.”

The text “In the top plot, black arrows representing wind speeds over 50 km h⁻¹ are present. In the bottom plot, these arrows are replaced with wind speeds 6-8 km h⁻¹ lower. The empirically-corrected data appears to match the stationary measurements better in tail wind, but still experiences difficulty with direction.” has been removed.

20. P13 L15 – I understand that CFD cannot simulate this but it could use a clearer explanation.

The text has been replaced with: “Field measurements were the only method of obtaining data under tail wind conditions in our study. Our CFD model was limited to a single inlet, and did not have the capability to simultaneously model oncoming air from the vehicle’s motion, and wind blowing from behind the truck.”

21. P13 L26 – Why is there more variability in tailwind conditions? Please explain for readers.

[Printer-friendly version](#)[Discussion paper](#)

This comment is addressed in the next detailed comment response.

22. P13 L30 – Perhaps this could be better explain – the tail wind will be ‘embedded’ in the flow around the vehicle in real-world conditions, so why wouldn’t it be ‘detected’?

We have added the bolded text in at P13 L30 to address detailed comments 21 and 22 together, into the paragraph beginning at P13 L24. The text has been changed to:

“The plotted wind vectors in Fig. 8 show that the 1 Hz mobile wind measurements experience the most variability in speed and direction when the vehicle is travelling in tail wind conditions. The empirically corrected tail wind direction measurements were in reasonable (within $\sim 30^\circ$) agreement with stationary direction measurements on field days with winds greater than 25 km h⁻¹, but deviated on days with lower wind speeds. When the vehicle speed is much larger than the wind speed, the vehicle creates a continuous flow field that can obstruct natural winds. The anemometer detects continuous frontal wind from the vehicle, and becomes less sensitive to components of the wind coming from behind the vehicle. It is likely that a windspeed threshold for the magnitude of tail wind detected by the mobile anemometer, and that this threshold varies with vehicle speed. Additional field testing on field days with low winds is recommended to evaluate the quality of tail wind measurements, identify windspeed thresholds, and develop quality control criteria for tail wind measurements. As CFD is limited in developing an empirical correction for tail wind, additional field data is recommended to develop a correction for tail wind measurements.

23. P14 L1 – Should be ‘mobile anemometers’

This change has been made.

24. P14 L1 – Not sure where the ‘mean’ was compared. Please expand on this.

We have moved the text, “The results are displayed in Table 3.” From P14 L4 to P14 L2 to draw attention to Table 3 which compares the percent difference between mean short and tall anemometer measurements across vehicle speed.

Printer-friendly version

Discussion paper



25. P14 L7 – What about other uses of mobile wind data? How would this improve a meteorological field study, for example?

In the discussion we have added the statement, “Vehicles outfitted to study severe weather (Curry et al., 2017; Taylor et al., 2011), and urban meteorology (Joe et al., 2018) show resilience to bias by also outfitting vehicles with wind sensors above and ahead of the vehicle.”

This comment is also addressed in the response to the detailed comment below.

26. P15 L20 – On a daily basis? Only during field studies?

The following text has been added to P15 L24

“Vehicle-based wind measurements from field studies can be used to contribute to detailed observing networks of specific sites. Furthermore, vehicle-based wind measurements can be collected conveniently by vessels of opportunity that travel routine routes, and contribute to weather data assimilation to evaluate accuracy for air quality and weather forecasting models (Brook et al., 2013).

27. P15 L30 – But what is the representative height being aimed for? You could try to install at 20 m mast and it would certainly be out of the vehicle envelope, but do you want to know the winds at that height? The authors have not made it clear at what height stakeholders require wind data.

P15 L32 has been modified to:

“For applications requiring near surface wind measurements to be paired with other vehicle-based measurements, and similar anemometer placements to those in this study, we recommend anemometers on truck caps be mounted at least 1 m above the vehicle, and that an empirical correction be applied. While mounting the anemometer at larger heights above the vehicle reduces the impact of flow distortion resultant from the vehicle’s motion, placement must be practical and safe for road travel. For larger vehicle’s, we expect mounting anemometers on vehicle’s at heights much greater than

Printer-friendly version

Discussion paper



1 m to be potentially impractical. It is important that placement keeps the sensor below common road clearance limits for bridges and underpasses.”

Interactive comment on Atmos. Meas. Tech. Discuss., doi:10.5194/amt-2018-354, 2018.

[Printer-friendly version](#)

[Discussion paper](#)



Using computational fluid dynamics and field experiments to improve vehicle-based wind measurements for environmental monitoring.

Tara Hanlon¹ and Dave Risk¹

¹Department of Earth Sciences, St. Francis Xavier University, Antigonish, Nova Scotia, B2G 2W5, Canada

Correspondence: Tara Hanlon (thanlon@stfx.ca)

Abstract. Vehicle-based measurements of wind speed and direction are presently used for a range of applications, including gas plume detection. Many applications use mobile wind measurements without knowledge of the limitations and accuracy of the mobile measurement system. Our research objective for this field-simulation study was to understand how anemometer placement and the vehicle's external air flow field affect measurement accuracy of vehicle-mounted anemometers. Computational Fluid Dynamic (CFD) simulations were generated in Ansys FLUENT to model the external flow field of a research truck under varying vehicle speed and wind yaw angle. The CFD simulations provided a quantitative description of fluid flow surrounding the vehicle, and demonstrated that the change in windspeed magnitude from the inlet increased as the wind yaw angle between the inlet and the vehicle's longitudinal axis increased. The CFD results were used to develop empirical speed correction factors at specified yaw angles, and to derive an aerodynamics-based correction function calibrated for wind yaw angle and anemometer placement. For comparison with CFD, we designed field tests on a square, 12.8 km route in flat, treeless terrain with stationary sonic anemometers positioned at each corner. The route was driven in replicate under varying wind conditions and vehicle speeds. The vehicle-based anemometer measurements were corrected to remove the vehicle speed and course vector. From the field trials, we observed that vehicle-based windspeed measurements differed in average magnitude in each of the upwind, downwind, and crosswind directions. The difference from stationary anemometers increased as the yaw angle between the wind direction and the truck's longitudinal axis increased, confirming the vehicle's impact on the surrounding flow field and validating the trends in CFD. To further explore the accuracy of CFD, we applied the function derived from the simulations to the field data, and again compared these with stationary measurements. From this study, we were able to make recommendations for anemometer placement, demonstrate the importance of applying aerodynamics-based correction factors to vehicle-based wind measurements, and identify ways to improve the empirical aerodynamic-based correction factors.

1 Introduction

Many scientific applications require local measurements of wind speed and direction in the lower atmosphere. Currently, vehicle-based wind measurements are used to study [severe weather-related](#) meteorology (Belušić et al., 2014; Straka et al., 1996), [lake meteorology](#) (Brook et al., 2013; Curry et al., 2017), and are integrated into methane measurement studies to detect, 5 quantify, and map emission plumes from oil and gas developments (Atherton et al., 2017; Rella et al., 2015; Zazzeri et al., 2015).

Existing mobile measurement platforms include car, sport utility vehicle (SUV), and truck-mounted anemometers, although the quality and accuracy of the anemometer measurements is not well understood. As a vehicle travels, its motion creates an air flow field that is unique to the shape and velocity of the vehicle. To avoid measurement bias, instruments measuring wind 10 speed and direction must be placed in a location that is not directly impacted by the flow and pressure perturbation produced by the moving vehicle (Straka et al., 1996). Mobile platforms often mount sensors in locations ahead of or above the vehicle (Atherton et al., 2017; Belušić et al., 2014; Raab and Mayr, 2008; Rella et al., 2015; Zazzeri et al., 2015). In the development of a mobile mesonet fleet (Straka et al., 1996), the importance of placing wind sensors outside of the vehicle's flow field was referenced, and the authors obtained wind tunnel tests from Nissan to determine the sensor placement. Another study (Raab and 15 Mayr, 2008) mounted an anemometer atop a car, referencing that Computational Fluid Dynamic (CFD) analysis performed by car manufacturers showed the flow disturbance caused by a car was minimal near the car's frontal axle, at a height equivalent to one metre above the roof. These studies provide reasoning for sensor placement, but lack empirical study or simulation and quantitative understanding of the flow field to confirm that the measurements were indeed not impacted by the vehicle's flow and pressure perturbation. Smart sensor placement will reduce measurement bias, but measurements should also be calibrated 20 for the bias to generate better accuracy, and greater certainty, of vehicle-based wind measurements.

The majority of studies evaluating the external flow field of vehicles do so for the purpose of evaluating aerodynamic drag (Yang and Khalighi, 2005; Holloway et al., 2009). In these studies, the spatial resolution around the vehicle is too limited to represent the complex flow field detail, and areas of flow separation cannot be identified (Defraeye et al., 2010). For the purpose of evaluating bias of a wind sensor measurement atop the vehicle, improved resolution is needed. Houston et al. (2016) 25 recognized this problem, and created CFD simulations to evaluate the wind field at the location of wind sensors mounted atop a Dodge Caravan, finding that the vehicle caused the windspeed at the sensor locations to be overestimated by 4% in head wind, and could exceed overestimations of 9% in cross wind. Marine researchers have already conducted similar experiments, which led to correction functions for shipboard anemometers (Moat et al., 2005; Yelland et al., 1998). The shape of the ship's hull and the oscillating motion of the vessel distort airflow, causing a bias in wind measurements that is unique to the location of the 30 anemometer (Moat et al., 2005). CFD and wind tunnel studies on Canadian research ships show that the anemometers placed ahead of the bow underestimate windspeed, whereas anemometers mounted on the main mast overestimate the windspeed (Moat et al., 2005). Wind tunnel studies show that the bow-positioned anemometers underestimate windspeed by a magnitude of three to five percent, while those at the main mast overestimate windspeed by a magnitude of five to ten percent (Thiebaux, 1990). In comparison, CFD studies indicate that anemometers positioned on the bow may decelerate the flow between 0 and

15 percent, while those at the main mast overestimate by approximately 5 percent (Yelland et al., 1998). Similar experiments have not been conducted for truck-based anemometers.

In this study, we set out to quantify truck-based anemometer measurement bias, and to derive an integrative placement and empirical calibration solution for vehicle-based anemometer measurements on a specific research vehicle. We used synthetic data from computational fluid dynamic simulations to obtain a spatial description of the behaviour of the flow field surrounding the vehicle, over a large range of vehicle speeds and wind yaw angles. The synthetically derived corrections were compared with field measurements acquired using a truck-mounted anemometer at multiple placements, with varying truck speeds and wind yaw angles. By evaluating the vehicle's external flow field under both varying vehicle speed and wind yaw angle we can quantify the bias the vehicle shape induces on a truck mounted anemometer and calibrate the measurements prior to correcting wind speed and direction measurements for the vehicle's motion.

2 Methods

2.1 CFD Study

CFD simulations were used to develop a quantitative understanding of fluid flow around the vehicle, and to evaluate flow under a wider range of conditions than is feasible in a field study. These data were used to investigate how the shape of the vehicle impacted measurement accuracy when the vehicle was travelling in the upwind and crosswind directions. We defined measurement bias as the difference between the inlet velocity and the velocity magnitude at the anemometer location. We created two sets of simulations in ANSYS FLUENT, the first of which was designed to evaluate the flow field under varying vehicle speed, and the second to explore the flow field under varying wind yaw angles.

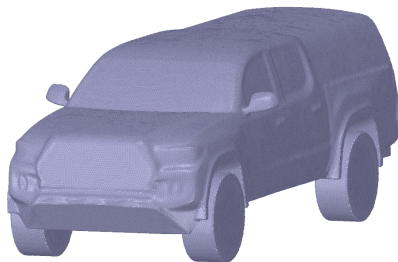


Figure 1. Truck model geometry replicating a 2016 Toyota Tacoma field vehicle.

The vehicle geometry was that of a 2016 Toyota Tacoma model equipped with a bed cap cover, similar to that used in Atherton et al. (2017), and modified to have a smooth underbody with simplified tires. The vehicle model (Fig. 1) was enclosed in a virtual wind tunnel extending 25.4 m above, ahead, behind, left, and right of the truck model. The computational domain

of the wind tunnel was 56.2 m in length, 53.0 m in width, and 28.2 m in height, with just under 84 000 m³ of air volume. The wind tunnel was designed to have a large width so that the vehicle speed and yaw angle could be evaluated in a consistent manner across simulations. A fine resolution tetrahedron assembly mesh was generated in the ANSYS workbench package with 4.6 million cells, ranging from fine-scale adjacent to the surface of the truck to coarse farther away. The computational wind tunnel was defined to have a velocity based inlet (1% turbulence intensity), and a pressure based outlet. We modelled the road and truck surfaces as stationary walls with no slip condition, and the top and sides of the tunnel with symmetry boundary conditions.

A drag coefficient comparison with the manufacturer's specification was used to compare the performance of three turbulence models. We calculated the drag coefficient of the truck model using a realizable two equation k- ϵ model with non-equilibrium wall functions, a two equation k- ω shear stress transport (SST) model, and a four equation transition SST model. All turbulence models are built into the ANSYS software and based on the steady state formulation, Reynolds Average Navier Stokes (RANS) equations. In simulations comparing the turbulence models, the drag coefficient was calculated using an inlet velocity of ~~22.222~~ 22.2 m s⁻¹ (80 km h⁻¹), and the vehicle's projected frontal area of 2.819 m². The drag coefficient was determined when the change in C_D was less than 0.001. The ΔC_D column was determined by comparing the calculated drag with the 2016 4x4 Double Cab Toyota Tacoma specification value for C_D of 0.386 (Toyota USA, 2016). The results of the C_D comparison are displayed in Table 1. All turbulence models produced drag coefficients greater than the manufacturer's reported value. The addition of the cap on the truck model may have increased the frontal area, resulting in this slightly larger drag coefficient. The k- ϵ model provided a C_D value within 6% of Toyota's specification value, and was chosen as the most suitable model for our computational mesh.

Previous studies (Holloway et al., 2009; Roy and Srinivasan, 2000; Yang and Khalighi, 2005) have used k- ϵ models for the purpose of external vehicle aerodynamics. The k- ϵ models use two additional equations to solve the RANS equations, one for turbulent kinetic energy (k) and one for the turbulent kinetic energy dissipation rate (ϵ) (Roy and Srinivasan, 2000). The realizable k- ϵ model with non-equilibrium wall functions was advantageous for this study. Non-equilibrium wall functions are sensitized to adverse pressure gradients and predict flow behaviour in turbulent boundary layers better than the traditional k- ϵ model, which is limited in cases of larger adverse pressure gradients (Parab et al., 2014). The k- ϵ model has been previously used to study external vehicle aerodynamics. Holloway et al. (2009) compared a steady k- ϵ model with two transient turbulence models, concluding that all of the models capture the general trends in the flow field aft of the cab of a pickup truck. In a study comparing CFD and experimental data, similar flow structures were observed from a steady k- ϵ CFD model and time averaged wind tunnel test experiments when comparing velocity planes parallel to the ground (Yang and Khalighi, 2005). The pickup truck models in both these studies had an open bed. In our study, the model we were exploring has a cap on the bed. The flow field around a pickup truck is more complex ~~and unsteady~~ than the flow field around an SUV or sedan because of ~~the wake flow interactions with the open box~~ wake interactions (Yang and Khalighi, 2005). The cap on the truck bed eliminates the pressure drop that occurs on pickup trucks when the air flows over the cabin and into the bed. Our ~~area of interest, the flow atop the cap of the vehicle, is located away from large pressure gradients. Because the cap eliminates large pressure gradients at the area of interest~~ motivation for placing an anemometer atop a pickup came to assist vehicle-based gas monitoring systems

Table 1. Drag comparison of three turbulence models with inlet velocity of $22.222\text{--}22.2\text{ m s}^{-1}$. Δ The drag coefficient (C_D values are calculated) for each turbulence model is reported with respect the number of iterations required to Toyota achieve a solution and the percent difference (ΔC_D) from the manufacturers reported (C_D) of 0.386 the vehicle model.

Turbulence Model	Iterations	C_D	ΔC_D
k- ϵ	436	0.411	6 %
k- ω	234	0.417	8 %
SST	217	0.446	15 %

(Atherton et al., 2017; Baillie et al., 2019; O’Connell et al., 2019) measuring gas emissions to achieve practical placement and further calibration practices. In these studies, the anemometer was mounted above a truck cap. Because of the differing vehicle shape from an open bed pickup truck, k- ϵ performance in the drag comparison, and its results performance in other studies, we have selected the k- ϵ turbulence model as appropriate for our analysis in the velocity field above a capped pickup truck.

In the first set of simulations, the above model was used to investigate the flow over the vehicle at speeds ranging from 40 to 100 km h⁻¹ in 5 km h⁻¹ increments. All simulations were performed in ANSYS Fluent 17.2, and were run in parallel using 32 cores dispersed over two nodes using 2.2 GHz Operton or Intel Xeon 2.7 GHz clusters made available by Compute Canada.

In the second set of simulations, eight additional computational domains were created to explore the effects of wind yaw angle, each representing a different wind yaw angle for the truck. In each case, the truck’s longitudinal axis was rotated so that the inlet was perpendicular to the yaw angle direction of flow. The computational domain was to made to extend the same 25.4 m in each direction as the original tunnel. The truck was rotated counterclockwise in 5° increments to provide models between 5° and 40°, inclusive. The symmetry plane of the truck was used to simulate the corresponding yaw angles of 320° to 355°, inclusive. We assumed that the wind atop the truck on the passenger side at 5° will represent the same wind that the driver side of the truck experiences if the truck was rotated 355°. We used the additional computational domains to test all combinations of yaw and inlet speed under inlet speeds ranging from 40 km h⁻¹ to 100 km h⁻¹ in 5 km h⁻¹ increments.

2.2 Field Measurements

The field experiments were designed to validate the CFD results, using stationary anemometer measurements as a control comparison for truck-based anemometer measurements. For comparison with CFD, it was necessary to obtain truck-based wind measurements from a range of yaw angles. Field tests were carried out using a 3.2 km by 3.2 km driving route, with a stationary anemometer positioned near each corner in order to compare truck-based anemometer measurements under head wind, tail wind, and side wind conditions, with those acquired by the stationary anemometers. The stationary anemometers were placed on the corners to provide opportunity for comparison with both legs of the straightaway. This ensured that we would have data for comparison with each leg should an anemometer malfunction. The square route also provided vehicle-based measurements for tail wind conditions, where stationary anemometers recorded wind direction opposing the vehicle

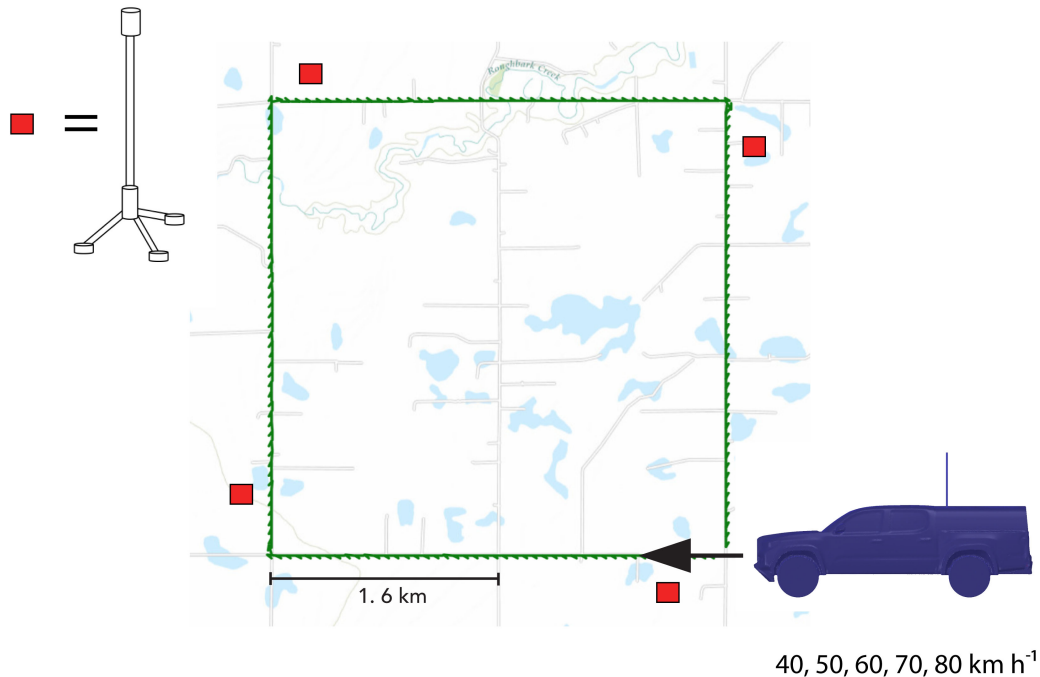


Figure 2. Field schematic displaying the location of stationary anemometers, the site, and the vehicle path. The vehicle path was driven clockwise and repeated at speeds of 40, 50, 60, 70, and 80 km h⁻¹.

path. The ~~CFD study did not obtain results from conditions where the wind direction was opposing the frontal wind from the vehicle.~~ The terrain was flat, treeless, nearly devoid of infrastructure, and we experienced minimal traffic.

5 In summer 2017, we drove the route at speeds of 40, 50, 60, 70, and 80 km h⁻¹. Our hardware consisted of an RM Young 86004 ultrasonic anemometer mounted on a 1.2 m tall mast above the cap of a 2016 Toyota Tacoma, with a total height of 3 m above the surface. The anemometer was positioned 0.5 m from the longitudinal axis of the truck on the driver's side, and 0.3 m behind the start of the truck's cap, in the location of the roof racks. A Campbell Scientific CR1000x datalogger recorded time, wind speed, wind direction, and instantaneous geolocation from a Garmin GPS 18X, at 1 Hz. Four stationary tripod-mounted
 10 Decagon Device DS-2 sonic anemometers measured wind speed and wind direction at a height of 3 m above the ground. The tripods were located approximately 300 m clockwise from each corner. Measurements of time, wind speed, maximum gust, and direction were recorded with a Decagon Device Em50 datalogger in one minute intervals at the same time we were driving the route. A schematic describing the field experiment is displayed in Fig. 2.

To explore the effects of the anemometer height above the truck, we also repeated tests using a secondary lower position of
 15 0.3 m above the truck (2.1 m above the ground), and 0.4 m from the longitudinal axis of the truck on the driver's side.

The ~~vehicle~~ 1Hz geolocation measurements were used to compute the vehicle speed and bearing, field measurements that deviated more than 2.5 km h⁻¹ from the implemented cruise control speed, vehicle bearing measurements that differed more

than 5° from designated vehicle course were removed from the data set. The vehicle anemometer measurements from each field test were corrected to remove the vector of the vehicle's motion. ~~The vehicle speed and bearing were calculated from the 1 Hz GPS position measurements~~ To correctly compute true winds, vehicle based wind must be corrected for the vehicle's motion over the fixed earth. The vehicle vector has a direction equivalent to the vehicle's course over the ground, and a magnitude equivalent to the vehicle's speed over the ground (Smith et al., 1999). The 1 Hz wind direction and wind speed measurements from the truck anemometer were each used to create the real and imaginary components for the wind vector, with the coordinate system aligned so that the front of the truck was 0 degrees. The wind vector was translated to match the truck's coordinate system, with North as 0 degrees, ~~and a true wind vector was computed by removing the vehicle.~~ We calculated the vehicle's course over the ground using the 1 Hz GPS coordinates to obtain a vector ~~from the~~ of equal magnitude and opposite direction to be the frontal wind induced by the vehicle ~~wind vector.~~ All computations were completed using R 3.4.1 statistical software (R Core Team, 2016)'s motion (F). We compute the meteorological wind vector (W) by subtracting the frontal wind induced by the vehicle's motion (F) from the raw anemometer measured wind vector (A). The calculation is presented in Equation (1). The computation comes from the method calculating the meteorological true wind from a moving vessel presented by Smith et al. (1999).

$$W = A - F \tag{1}$$

3 Results and Discussion

The CFD simulations and field experiments show that vehicle-based anemometers are subject to bias as a result of the vehicle's flow field. The CFD and field experiments showed ~~similar qualitative trends.~~ that the measured wind at the anemometer location varied under wind yaw angle. The bias found in the CFD varied with the rotation of the truck, and the field results concluded that the measured wind differed in head, cross and tail wind conditions. We first present the CFD results, followed by those from the field.

3.1 CFD results

The CFD simulations provided a quantitative description of the air flow surrounding the vehicle. Velocity fields were the interest of this study, and we observed that wind yaw angle has a more pronounced effect on the wind speed bias than the vehicle speed does. The first set of simulations was evaluated to explore the effect of vehicle speed on wind measurement bias. ~~We~~ In each computational domain, we found that the wind bias scaled with vehicle speed, ~~as the relationship between windspeed at specified locations was linear with increasing vehicle speed,~~ and the amount of bias (slope) ~~was specific to the anemometer location~~ differed with the location above the vehicle. Similarly, Houston et al. (2016) found that CFD calculated velocities for sensors positioned atop a van scaled linearly with along axis speed. Our location of interest for placing anemometers was on the truck's bed cap. Velocity contours were computed for the longitudinal axis of the truck, and for the lateral plane on the

truck located 30 cm from the end of the cab, which was the location of the roof racks on which the anemometers were mounted in the field test.

Figure 3 displays a velocity contour for the overestimation of the speed along the longitudinal axis of the truck. In this plane, we found that the velocity flowing over the truck was less than the inlet speed at small heights above the truck cabin and cap. In the location of the roof racks, the flow velocity was less than the inlet speed at heights lower than 17 cm above the truck. At 17 cm, the velocity flow transitioned to become larger than the inlet speed. The velocity gradient with respect to height was largest in the region where the flow transitioned to becoming larger than the normalized wind speed, and decreased with increasing height. The magnitude of flow acceleration was greatest immediately above 17 cm, and decreased with increasing height above the truck. This observation is similar to a conclusion by Moat et al. (2005), stating that shipboard anemometers should not be placed close to the line of equality (where measured windspeed = true windspeed) as high pressure gradients are present in this region. The line of equality would be expected to move vertically to some degree, according to the ground speed and/or windspeed.

The second set of simulations in this study are of particular interest ~~as we lack~~ because they evaluate the flow field under cross wind conditions. Many previous CFD and wind tunnel tests examining the flow fields resulting from non-perpendicular air flow to the front studies (Holloway et al., 2009; Yang and Khalighi, 2005) examine the flow field resulting from inlets which direct the airflow along the longitudinal axis of the vehicle. Aside from Houston et al. (2016), we have not found studies using CFD to conduct crosswind experiments to study the flow field around a vehicle. In performing this analysis, we observed that the change in windspeed magnitude from the inlet increased along with the wind yaw angle between the inlet and the vehicle's longitudinal axis. The flow above the truck displayed a profile where decelerating flow was found below a region of accelerating flow before reaching the undisturbed velocity flow. The maximum magnitude of flow acceleration that occurs above the deceleration region increased with increasing yaw angle. Figure 4 shows the profile of velocity contours in the lateral plane of the truck, along the location of the roof racks on the truck when the truck is exposed to frontal, 15° passenger, and 30° passenger wind. When exposed to large yaw angles, the wind bias over the truck at low heights can be twenty percent, and even at significant heights a height of 1.7 m above the vehicle, a bias of greater than 5 percent is present.

Anemometers must be placed away from the region of sharp velocity gradients to avoid wind bias. The height of this region changes based on the angle at which the wind is flowing over the truck. From the velocity profiles, we conclude that anemometers measuring wind speed and direction must be mounted at a significant height above the vehicle. For the velocity profile of the longitudinal axis of the truck, we found that the flow differential dropped below 2% at a height of 2.59 m above the truck and below 1% of the inlet speed at a height of 4.36 m above the truck. These heights are displayed in Fig. 3. Looking at the longitudinal velocity profile located 50 cm left of the truck's axis, we found that the flow acceleration dropped below 2% of the inlet speed at a height of 2.61 m above the truck, and below 1% of the inlet speed at a height of 4.47 m above the truck. From this, we can conclude that an anemometer mounted off the centre line must be positioned higher than one mounted in the centre of the truck. Furthermore, we found that the wind yaw angle was critical for determining the height at which to mount a sensor atop a vehicle. Table 2 shows the minimum height required to mount a sensor where the flow acceleration is less than 2% for an anemometer mounted on the longitudinal axis of the truck, 0.3 m behind the truck cab. It is expected that the bias of

less than 2% would fall within sensor accuracy. The RM Young anemometer used in our field experiment had an accuracy of 2% for speeds of less than 30 m/s, and 3% for speeds between 30 and 70 m/s.

Anemometer placement should not be determined from wind tunnel tests with directly frontal flow. Table 2 shows that a ~~frontal wind tunnel test could give a false height suitable for anemometer placement. The height above the truck where the bias resulting from the vehicle's shape becomes negligible increases with the height required for an anemometer to experience bias below 2% increases with increasing~~ yaw angle. Anemometer heights selected through frontal wind tunnel tests would still experience bias under cross wind conditions. It is expected that vehicle-mounted anemometers would be subject to yaw angles between 0° and 40° . For perspective, if a vehicle was driving at 80 km h^{-1} perpendicular to a wind of 22 km h^{-1} , the apparent yaw is expected to be 15 degrees. In days with high winds and low driving speeds, it is possible to experience a yaw angle of 40 degrees. The bias experienced at the anemometer height in our field tests is greater than the instrument accuracy, therefore we must correct anemometer measurements for flow distortion.

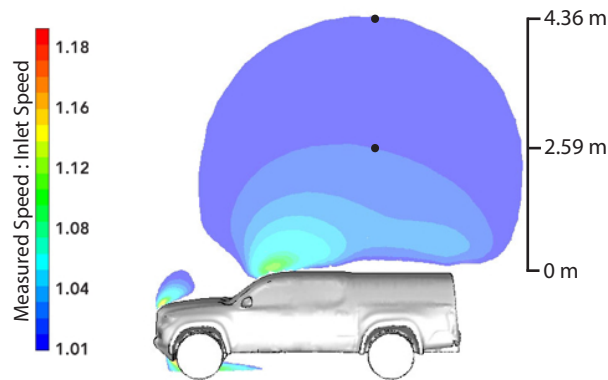


Figure 3. Frontal wind velocity contour of the truck's longitudinal axis. The black dot at 2.59 m represents the anemometer height required to be subject to less than 2% bias, and the black dot at 4.36 m represents the anemometer height required to be subject to less than 1 % bias, if mounted 30 cm behind the truck cab.

We derived aerodynamic-based correction factors to be applied to vehicle-based wind measurements from the simulation datasets. The normalized ~~windspeed~~ wind speed (measured wind speed: inlet speed) at the location of an anemometer mounted in the same location as the field test was computed for each yaw angle simulation. The empirical correction factor for each yaw angle is the reciprocal of the normalized windspeed. Empirical correction factors were computed for the anemometer placement in the field trials, and for an anemometer placement in the centre of the truck, above the roof racks. The correction factors for both anemometer placements were fitted with weighted polynomial regressions. Figure 5 shows the function for both placements. The centred placement provides a symmetrical function, whereas the side-mounted anemometer measures lower windspeed coming from the driver side than the passenger side. The wind coming from yaw angles over the passenger side experiences similar bias in both placements. We conclude that, by moving the anemometer to the side of the truck, we reduce the

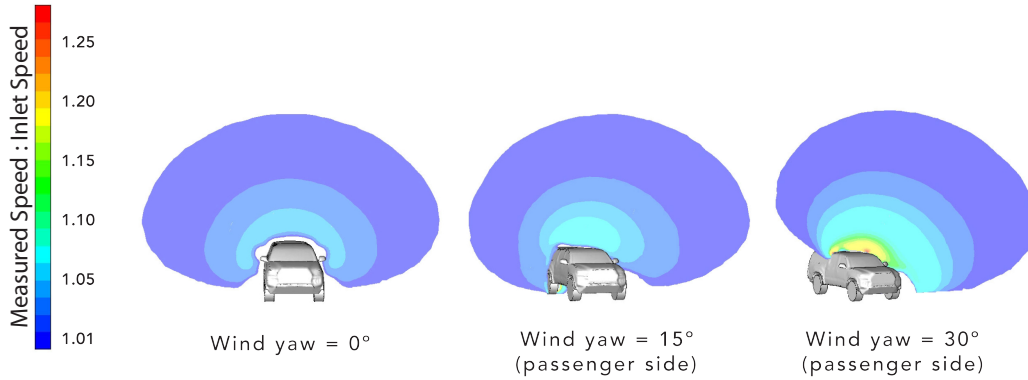


Figure 4. Velocity contours of the lateral plane of the truck along the roof racks for yaw angles of 0°, 15°, and 30°. Yellow regions indicate that the wind is accelerated by 18%.

Table 2. Required anemometer height for a centrally-mounted anemometer to experience negligible bias.

Yaw Angle	Height
0°	2.59
5 °	2.67
10°	2.87
15°	3.01
20°	3.28
25°	3.48
30°	3.73
35°	3.92
40°	4.04

bias from wind yaw angles experienced on the driver side. Figure 5 shows that it is important that the anemometer correction function is calibrated for the anemometer placement. The [polynomial pictured in Fig 5 is multiplied by the Anemometer windspeed \(\$A_{WS}\$ \), to give the corrected wind speed \(WS\). Equation 2 gives the side-mounted anemometer’s correction function is:](#)

$$WS = 9.6286(10^{-1}) - 1.4166(10^{-4})WD - 5.5849(10^{-5})WD^2 + 9.7413 * (10^{-8})WD^3 + 1.5485(10^{-8})WD^4$$

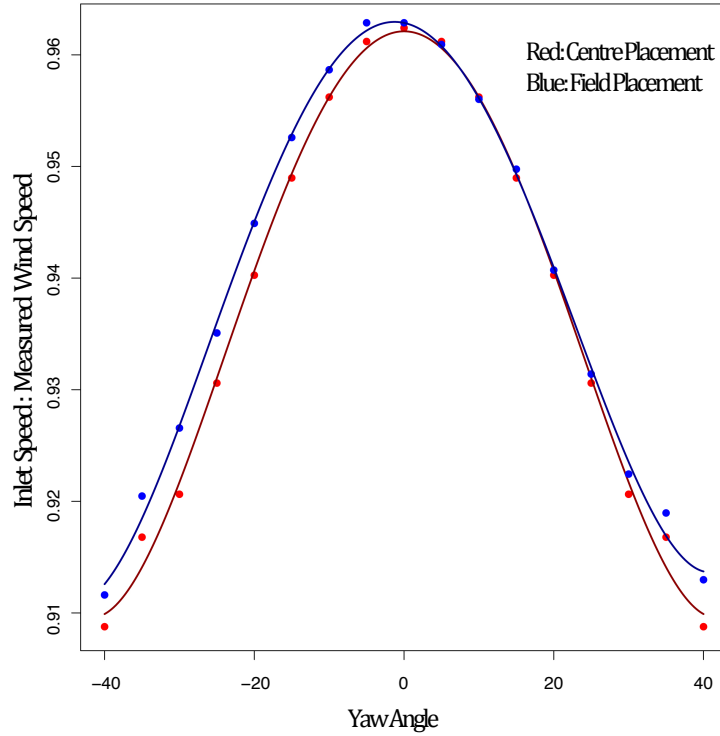


Figure 5. Empirical correction factors for field placement (blue) and centred placement (red) fitted with weighted polynomial regression.

Where $WS = \text{Windspeed}$, $WD = \text{Wind Direction}$, and for wind direction (WD) measurements ranging from $-40^\circ < WD < 40^\circ$. Wind speed units are in km h^{-1} and wind direction units are in degrees.

$$WS = A_{WS} \times (9.6286(10^{-1}) - 1.4166(10^{-4})WD - 5.5849(10^{-5})WD^2 + 9.7413(10^{-8})WD^3 + 1.5485(10^{-8})WD^4) \quad (2)$$

The side-mounted anemometer placement was used in our field tests. For our field analysis, we will use Eq.(42) as an empirical correction function calibrated for anemometer placement and wind yaw angle. The empirical calibration must be applied to remove the bias of the vehicle's shape on anemometer measurements prior to correcting for the vehicle motion.

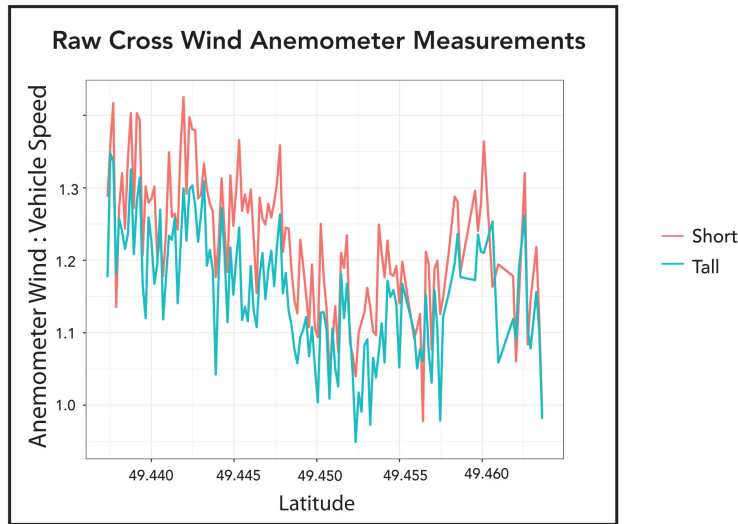


Figure 6. Comparison of short and tall anemometer measurements in cross wind.

3.2 Field Results

The field results provided true measurements of the flow field at two locations above the truck. While the spatial resolution of the flow field was limited, the measurements were able to provide data true to the application.

To evaluate the vertical velocity profile, we compared the measurements from the two anemometer tests. The short anemometer measured larger mean wind speeds in the head, cross, and tail wind directions, demonstrating that vehicle speed had a greater impact on the windspeed measurements of the short anemometer. Figure 6 shows magnitude of the tall and short anemometer measurements sealed with when normalized by the vehicle speed. We concluded that vehicle speed had a larger effect on the short anemometer placement.

The field data was were compared with the stationary anemometers. For our results, we present the corrected field data in two ways: (1) with the frontal wind correction, and (2) with the applied CFD empirical correction, and then the frontal wind correction. We found that the application of the frontal wind correction overestimates windspeed in head wind, underestimates in tail wind, and differs in passenger side and driver side wind. Applying the CFD empirical correction reduces the overestimation in headwind and the underestimation in tail wind. It also improves the windspeed in passenger and driver side wind.

We found that applying the empirical correction reduces the windspeed measurement outliers, and reduces the standard deviation of the wind direction measurements. Figure 7 shows the distribution of wind measurements across vehicle bearing. Figure 7 displays field test data with the frontal wind correction (left), the field data with the empirical correction applied, followed by the frontal correction (centre), and the stationary measurements, with the vehicle bearing being that which the vehicle was driving when adjacent to that anemometer (right). Applying the empirical correction levels the reduces the difference in the mean of the wind direction measurements across the four vehicle bearings. The plots outline the areas the vehicle was driving

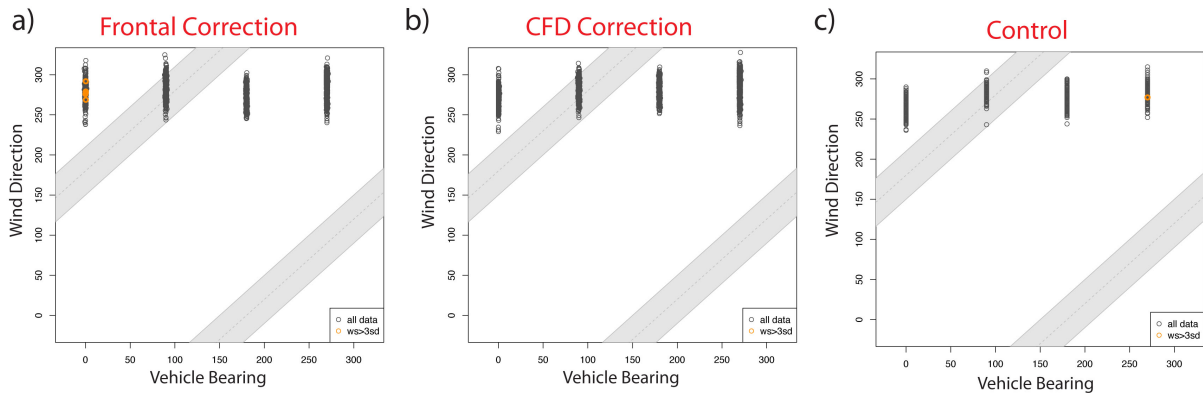


Figure 7. Distribution of wind measurements across vehicle bearing with (left) frontal correction applied to mobile measurements, (centre) empirical correction and frontal correction applied to mobile measurements, and (right) stationary measurements. [The shaded grey bars represent measurements acquired when the vehicle was driving in tail wind conditions. The yellow circles represent wind speed measurements that are greater than three standard deviations away from the mean wind speed of the wind speed measurements calculated with the a\) frontal correction applied, b\) empirical correction and frontal correction applied, and c\) specific to the stationary anemometer at each bearing.](#)

in tail wind, as we had expected more outliers to occur when driving in tail wind. The control plot shows that outliers can be expected due to the natural variability of the wind.

Figure 8 shows mapped vehicle wind vectors under the frontal (Fig. 8a) and empirical and frontal (Fig. 8b) corrections. Wind roses from the stationary anemometers on each leg are located in the corners. [The measurements in the wind roses are the wind gust and average wind direction measurements reported each minute of the 14 minute 60 km h⁻¹ speed test.](#)

[The mobile wind vector measurements in these plots are not averaged, and they were all taken when the vehicle was travelling within 2-2.5 km h⁻¹ of 70-60 km h⁻¹.](#) Both plots look similar, with the largest change being the reduction of the speed of the arrows in the empirical correction plot. [In the top plot, black arrows representing wind speeds over 50 km h⁻¹ are present. In the bottom plot, these arrows are replaced with wind speeds 6-8 km h⁻¹ lower. The empirically-corrected data appears to match the stationary measurements better in tail wind, but still experiences difficulty with direction.](#)

[Figures 7 and 8 demonstrate that measurement reliability and likely accuracy is improved by applying an empirical correction to vehicle anemometer measurements prior to correcting for the vehicle vector. The empirical correction from CFD improved the field measurements, but still could improve in tail wind.](#) [Figure 8 shows that applying the CFD calibration improves the agreement of the average mobile wind speed and direction measurements with the average stationary measurements in three of the four legs of the route.](#) Observations of windspeed as-measured (uncorrected for flow) show that when the truck was moving faster than 40 km h⁻¹, 72 % of raw wind direction measurements fell between -40 and 40 degrees of the front of the truck, the same as the yaw angles simulated in CFD. Field measurements [are the were the only](#) method of obtaining data [for under](#) tail wind conditions [, as CFD cannot simulate oncoming air both in front of and in our study. Our CFD model was limited to a single inlet, and did not have the capability to simultaneously model oncoming air from the vehicle's motion, and wind](#)

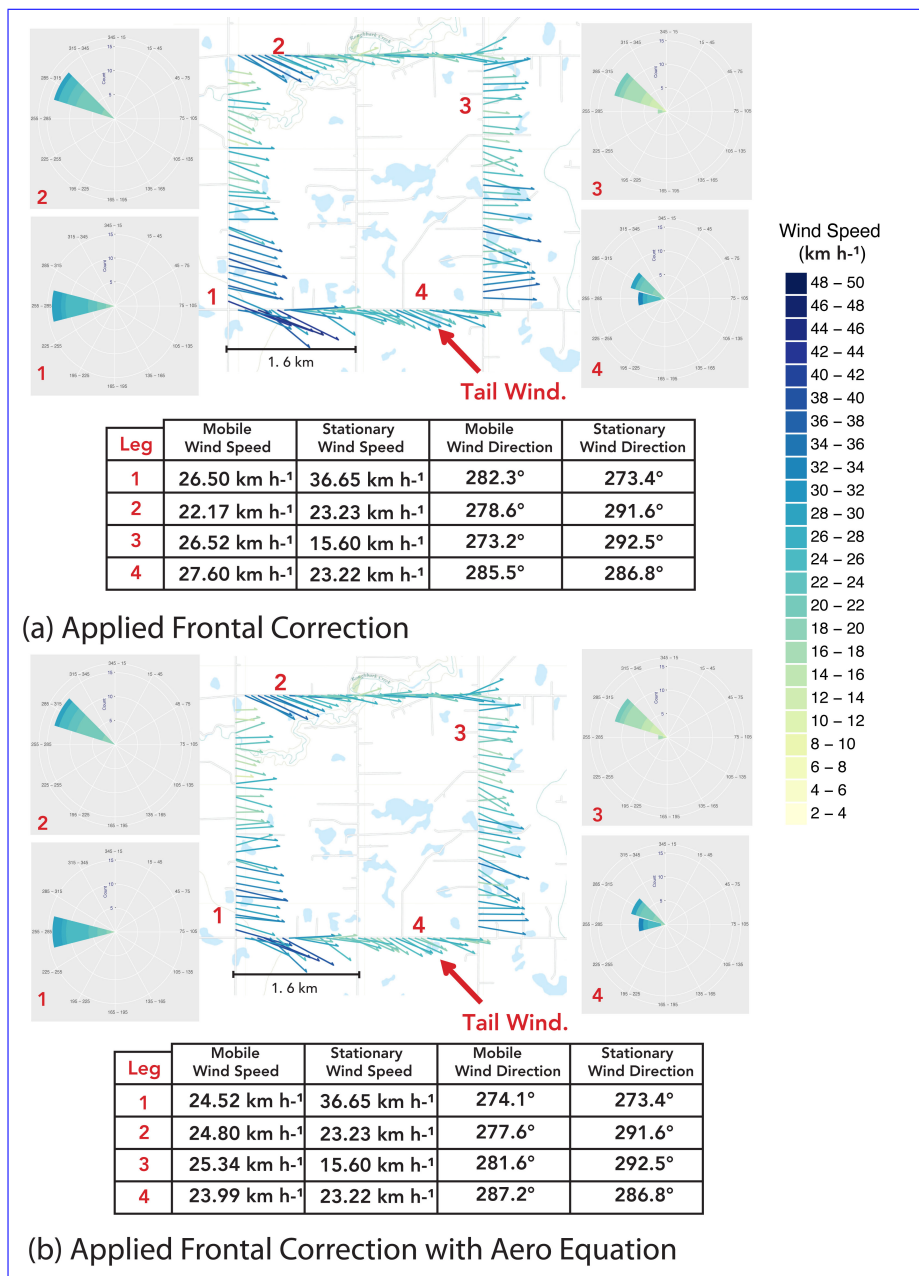


Figure 8. Mobile wind vectors displayed with adjacent stationary wind roses with a) frontal correction applied to mobile measurements, and b) empirical correction and frontal correction applied to mobile measurements.

[blowing from](#) behind the truck. Empirical correction factors could be derived from field experiments to provide better data for tail wind conditions. Our square experiment provided successful data for validation. The experiment could be expanded to include repetitive routes of each vehicle speed over a larger range of field days for exposure to more wind speeds. It would also

Table 3. Percent difference between mean short and tall anemometer measurements across vehicle speed.

Speed (km h ⁻¹)	Head Wind	Cross Wind	Tail Wind
50	0.0%	5.3%	6.6%
60	0.0%	5.7%	4.6%
70	2.1%	5.7%	10.2%
80	1.0%	5.2%	3.3%

be important to test on a day with little wind to identify a minimum wind speed to driving speed ratio for field practice. The resulting vehicle anemometer dataset with corresponding stationary measurements could be used to derive empirical correction factors. The data in our study only provided one square test per speed each day, and was unable to provide data at the range of yaw angles in which CFD was successful. However, square-route driving experiments would still be a good way to obtain a field-based empirical correction function, at least for the range of windspeed and wind yaw angle conditions experienced during the test.

We found that applying the CFD empirical correction function, followed by the frontal wind correction, reduced the number of wind speed outliers found on the square route. The plotted wind vectors in Fig. 8 show that the 1 Hz mobile wind measurements experience the most variability in speed and direction when the vehicle is travelling in tail wind conditions. The empirically corrected tail wind direction measurements were in reasonable (within ~30°) agreement with stationary direction measurements on field days with winds greater than 25 km h⁻¹, but deviated on days with lower wind speeds. In low wind, the continuous flow field from the vehicle can obstruct the wind coming from the opposite direction, and as a result the anemometer is unable to detect the tail wind, that can obstruct natural winds. The anemometer detects continuous frontal wind from the vehicle, and becomes less sensitive to components of the wind coming from behind the vehicle. It is likely that a windspeed threshold exists for the magnitude of tail wind detected by the mobile anemometer, and that this threshold varies with vehicle speed. Additional field testing on field days with low winds is recommended to evaluate the quality of tail wind measurements, identify windspeed thresholds, and develop quality control criteria for tail wind measurements. As CFD is limited in developing an empirical correction for tail wind, additional field data is recommended to develop a correction for tail wind measurements.

We applied the frontal wind correction to both mobile anemometers, and explored the difference in the mean windspeed at each vehicle speed in head, cross, and tail winds. The results are displayed in Table 3. The cross wind measurements used in this test were from the passenger side of the truck, as the post of the tall anemometer may have impacted the short anemometer measurements when the wind was coming from the driver side. The results are displayed in Table 3. The percent difference scales well across vehicle speed in head and cross winds. The agreement of the field measurements across vehicle speed shows that the wind speed scales linearly with vehicle speed and validates the trend in our CFD model. The measurements deviate in tail wind.

Wind bias from mobile anemometers could lead to volumetric error in methane emissions from oil and gas infrastructure. Plume dispersion applications feed wind measurements paired with gaseous concentrations from mobile measurement platforms into gaussian dispersion models to locate emitting infrastructure, estimate source emission rates, and quantify emitted volumes of methane in oil and gas developments (Atherton et al., 2017; Caulton et al., 2017). In the gaussian dispersion model, emission rate scales linearly with wind speed. Our CFD study has shown that the shape of the vehicle accelerates wind speeds between 3% and 10%, subject to wind yaw angle. When measuring downwind from infrastructure, the error in windspeed translates linearly to the error in calculated emission rate. Anemometer placement and measurement methodology should be assessed together to minimize potential wind bias prior to using wind measurements in dispersion models. Mobile surveying studies using trucks or sport utility vehicles (Atherton et al., 2017; Jackson et al., 2014; Phillips et al., 2013; Rella et al., 2015; Zazzeri et al., 2015) with anemometer placements above the vehicle are vulnerable to flow bias, and should use flow compensations to account for wind bias from the shape of the vehicle. Transect-based studies with anemometers placed atop sport utility vehicles (Caulton et al., 2017), should also apply flow compensations, although some transect-based studies using mobile laboratories (Roscioli et al., 2015; Yacovitch et al., 2015) with anemometers placed on a boom ahead of and above the vehicle are much more resilient to bias from the flow of the vehicle. Similarly, studies quantifying emissions in which the vehicle stops to obtain wind measurements (Brantley et al., 2014) and the anemometer is placed ahead of and above the vehicle, are unlikely to require compensations for the vehicle's flow field. [Vehicles outfitted to study severe weather \(Curry et al., 2017; Taylor et al., 2011\), and urban meteorology \(Joe et al., 2018\) show resilience to bias by also outfitting vehicles with wind sensors above and ahead of the vehicle.](#)

The calibration of vehicle-based measurements is important for integration with stationary measurements, and with mobile measurements from differing vehicle platforms. Studies evaluating the trends in near-surface ocean winds demonstrated that systematic bias in measurement methods attributed to an increasing trend in global windspeed in reported climate data (Cardone et al., 1990; Ramage, 1987; Peterson and Hasse, 1987). The International Comprehensive Ocean Atmosphere Data Sets (COADS) document wind measurements from Voluntary Observing Ships (VOS) and other marine platforms (Thomas et al., 2008). The datasets date back prior to the 1940s and provide data for observed changes in climate patterns (Ramage, 1987). The datasets have been studied extensively to explain the increasing trend in global wind speed after the 1940s (Cardone et al., 1990), when archived data prior to the 1940s showed a decreasing trend (Thomas et al., 2008). Peterson and Hasse (1987) and Ramage (1987) attributed the shift from decreasing to increasing wind speed to the change in the method of reporting ship-based wind measurements. The reported wind speeds range from estimated measurement based on sea state to recorded measurements from ship-mounted anemometers of varying height. The Beaufort Wind scale, a method for visually estimating the wind speed in relation to sea state characteristics, was introduced in 1946, and wind reports evolved from being derived from the amount of sail a ship could carry, to being derived from observation of sea state. The increasing trend after the 1940s has also been attributed to a change in measurement techniques, and to variation in anemometer height on ships. Peterson and Hasse (1987) found that as anemometers were introduced on research ships, the distribution of the reported Beaufort veloci-

ties changed significantly. The measurement of gust readings made available by anemometers influenced the estimation of the Beaufort force, as the values derived from sea state were reported to be higher. Thomas et al. (2008) attributed the gradual increase in average ship anemometer height as another contributor to the increase in mean windspeed. Thomas et al. (2005) compared wind reports from ships and buoys, and noted that ship winds were reported 25 % higher than buoy winds. Measured winds have subsequently been adjusted for height using a logarithmic profile, resulting in the measurements differing by only 6 %. While these adjustments were important, measured winds still are not calibrated for the acceleration or deceleration of flow in the anemometer location. Moat et al. (2005), Thiebaux (1990), and Yelland et al. (1998) indicated that ship-based anemometers are subject to bias between 0 and 15, with bow-placed anemometers on the lower end. Applying ship-based anemometer calibrations could further reduce the bias between ship and buoy winds.

Theoretically, vehicle-based measurements of wind speed and direction could be integrated with fixed site measurements to add spatial richness in climate, weather, and atmospheric observing systems. Our CFD results compare well with Houston et al. (2016) for sensor placements atop a vehicle, and suggest that flow compensations should be made for vehicle-based anemometers. Calibrating vehicle-based measurements for anemometer placement and vehicle shape make wind measurements comparable with adjusted weather station data, and can provide data to form an observing system of land-based surface winds. [Vehicle-based wind measurements from field studies can be used to contribute to detailed observing networks of specific sites. Furthermore, vehicle-based wind measurements can be collected conveniently by vessels of opportunity that travel routine routes, and contribute to weather data assimilation to evaluate accuracy for air quality and weather forecasting models \(Brook et al., 2013\).](#) To provide quality measurements, consistent processing techniques must also be developed to avoid systematic bias introduced by averaging and filtering.

5 Conclusions

Mobile measurement platforms are capable of providing spatial and temporal measurements of wind speed and direction. Vehicle-mounted anemometers are impacted by the vehicle's motion and the vehicle's flow field at the location of measurement. Increasing the height above the vehicle at which the sensor is mounted reduces the impact of the vehicle's flow field on measurements. Although the height required to completely eliminate the effect results in an impractically high position, empirical or CFD-derived corrections can help. For [applications requiring near surface wind measurements to be paired with other vehicle-based measurements, and](#) similar anemometer placements to those in this study, we recommend ~~that~~ anemometers on truck caps be mounted at least 1 m above the vehicle, and that an empirical correction be applied. [While mounting the anemometer at larger heights above the vehicle reduces the impact of flow distortion resultant from the vehicle's motion, placement must be practical and safe for road travel. For larger vehicle's, we expect mounting anemometers on vehicle's at heights much greater than 1 m to be potentially impractical. It is important that placement keeps the sensor below common road clearance limits for bridges and underpasses.](#) CFD and field methods are both appropriate methods for deriving corrections.

Data availability. TEXT

10 *Competing interests.* The authors declare they have no conflict of interest.

Acknowledgements. The authors would like to thank Nayani Jensen for her help in collecting field data. We would also like to thank Whitecap Energy staff and Andy Froncioni of Garmin International for their contributions that helped inspire and shape this study. This research was made possible with resources made available by ANSYS and Compute Canada.

References

- 15 Atherton, E., Risk, D., Fougère, C., Lavoie, M., Marshall, A., Werring, J., Williams, J. P., and Minions, C.: Mobile measurement of methane emissions from natural gas developments in Northeastern British Columbia, Canada, *Atmospheric Chemistry and Physics*, 17, 12 405, 2017.
- Baillie, J., Risk, D., Atherton, E., O'Connell, E., Fougère, C., Bourlon, E., and MacKay, K.: Methane emissions from conventional and unconventional oil and gas production sites in southeastern Saskatchewan, Canada, *Environmental Research Communications*, 1, 011 003, 2019.
- 20 Belušić, D., Lenschow, D., and Tapper, N.: Performance of a mobile car platform for mean wind and turbulence measurements, *Atmospheric Measurement Techniques*, 7, 1825–1837, 2014.
- Brantley, H. L., Thoma, E. D., Squier, W. C., Guven, B. B., and Lyon, D.: Assessment of methane emissions from oil and gas production pads using mobile measurements, *Environmental science & technology*, 48, 14 508–14 515, 2014.
- 25 Brook, J., Makar, P., Sills, D., Hayden, K., and McLaren, R.: Exploring the nature of air quality over southwestern Ontario: main findings from the Border Air Quality and Meteorology Study, *Atmospheric Chemistry and Physics*, 13, 10 461–10 482, 2013.
- Cardone, V. J., Greenwood, J. G., and Cane, M. A.: On trends in historical marine wind data, *Journal of Climate*, 3, 113–127, 1990.
- Caulton, D., Li, Q., Bou-Zeid, E., Lu, J., M. Lane, H., P. Fitts, J., Buchholz, B., Golston, L., Guo, X., McSpirtt, J., Pan, D., Wendt, L., and A. Zondlo, M.: Improving Mobile Platform Gaussian-Derived Emission Estimates Using Hierarchical Sampling and Large Eddy Simulation, pp. 1–39, 2017.
- 30 Curry, M., Hanesiak, J., Kehler, S., Sills, D. M., and Taylor, N. M.: Ground-based observations of the thermodynamic and kinematic properties of lake-breeze fronts in southern Manitoba, Canada, *Boundary-layer meteorology*, 163, 143–159, 2017.
- Defraeye, T., Blocken, B., Koninckx, E., Hespel, P., and Carmeliet, J.: Aerodynamic study of different cyclist positions: CFD analysis and full-scale wind-tunnel tests, *Journal of biomechanics*, 43, 1262–1268, 2010.
- 35 Holloway, S., Leylek, J. H., York, W. D., and Khalighi, B.: Aerodynamics of a pickup truck: combined CFD and experimental study, *SAE International Journal of Commercial Vehicles*, 2, 88–100, 2009.
- Houston, A. L., Laurence III, R. J., Nichols, T. W., Waugh, S., Argrow, B., and Ziegler, C. L.: Intercomparison of unmanned aircraftborne and mobile mesonet atmospheric sensors, *Journal of Atmospheric and Oceanic Technology*, 33, 1569–1582, 2016.
- Jackson, R. B., Down, A., Phillips, N. G., Ackley, R. C., Cook, C. W., Plata, D. L., and Zhao, K.: Natural gas pipeline leaks across Washington, DC, *Environmental science & technology*, 48, 2051–2058, 2014.
- Joe, P., Belair, S., Bernier, N., Bouchet, V., Brook, J., Brunet, D., Burrows, W., Charland, J.-P., Dehghan, A., Driedger, N., et al.: The Environment Canada Pan and ParaPan American Science Showcase Project, *Bulletin of the American Meteorological Society*, 99, 921–953, 2018.
- 5 Moat, B. I., Yelland, M. J., Pascal, R. W., and Molland, A. F.: An overview of the airflow distortion at anemometer sites on ships, *International Journal of Climatology*, 25, 997–1006, 2005.
- O'Connell, E., Risk, D., Atherton, E., Bourlon, E., Fougère, C., Baillie, J., Lowry, D., and Johnson, J.: Methane emissions from contrasting production regions within Alberta, Canada: Implications under incoming federal methane regulations, *Elem Sci Anth*, 7, 2019.
- 10 Parab, A., Sakarwala, A., Paste, B., Patil, V., and Mangrulkar, A.: Aerodynamic analysis of a car model using Fluent-Ansys 14.5, *International Journal of Recent Technologies in Mechanical and Electrical Engineering (IJRMEE) Volume*, 1, 2014.
- Peterson, E. and Hasse, L.: Did the Beaufort scale or the wind climate change?, *Journal of physical oceanography*, 17, 1071–1074, 1987.

- Phillips, N. G., Ackley, R., Crosson, E. R., Down, A., Hutyra, L. R., Brondfield, M., Karr, J. D., Zhao, K., and Jackson, R. B.: Mapping urban pipeline leaks: Methane leaks across Boston, *Environmental pollution*, 173, 1–4, 2013.
- R Core Team: R: A language and environment for statistical computing. R Foundation for Statistical Computing 2015, Vienna, Austria, 2016.
- Raab, T. and Mayr, G.: Hydraulic interpretation of the footprints of Sierra Nevada windstorms tracked with an automobile measurement system, *Journal of Applied Meteorology and Climatology*, 47, 2581–2599, 2008.
- Ramage, C.: Secular change in reported surface wind speeds over the ocean, *Journal of climate and applied meteorology*, 26, 525–528, 1987.
- 20 Rella, C. W., Tsai, T. R., Botkin, C. G., Crosson, E. R., and Steele, D.: Measuring emissions from oil and natural gas well pads using the mobile flux plane technique, *Environmental science & technology*, 49, 4742–4748, 2015.
- Roscioli, J., Yacovitch, T., Floerchinger, C., Mitchell, A., Tkacik, D., Subramanian, R., Martinez, D., Vaughn, T., Williams, L., Zimmerle, D., et al.: Measurements of methane emissions from natural gas gathering facilities and processing plants: measurement methods, *Atmospheric Measurement Techniques*, 8, 2017–2035, 2015.
- 25 Roy, S. and Srinivasan, P.: External flow analysis of a truck for drag reduction, Tech. rep., SAE Technical Paper, 2000.
- Smith, S. R., Bourassa, M. A., and Sharp, R. J.: Establishing more truth in true winds, *Journal of Atmospheric and Oceanic Technology*, 16, 939–952, 1999.
- Straka, J. M., Rasmussen, E. N., and Fredrickson, S. E.: A mobile mesonet for finescale meteorological observations, *Journal of Atmospheric and Oceanic Technology*, 13, 921–936, 1996.
- 30 Taylor, N. M., Sills, D. M., Hanesiak, J. M., Milbrandt, J. A., Smith, C. D., Strong, G. S., Skone, S. H., McCarthy, P. J., and Brimelow, J. C.: The Understanding Severe Thunderstorms and Alberta Boundary Layers Experiment (UNSTABLE) 2008, *Bulletin of the American Meteorological Society*, 92, 739–763, 2011.
- Thiebaut, M.: Wind tunnel experiments to determine correction functions for shipborne anemometers, *Can. Contractor Rep. Hydrogr. Ocean Sci.*, 36, 57, 1990.
- 440 Thomas, B. R., Kent, E. C., and Swail, V. R.: Methods to homogenize wind speeds from ships and buoys, *International Journal of Climatology*, 25, 979–995, 2005.
- Thomas, B. R., Kent, E. C., Swail, V. R., and Berry, D. I.: Trends in ship wind speeds adjusted for observation method and height, *International Journal of Climatology: A Journal of the Royal Meteorological Society*, 28, 747–763, 2008.
- Toyota USA: 2016 Toyota Product Information, 2016.
- 445 Yacovitch, T. I., Herndon, S. C., Pon, G., Kofler, J., Lyon, D., Zahniser, M. S., and Kolb, C. E.: Mobile laboratory observations of methane emissions in the Barnett Shale region, *Environmental science & technology*, 49, 7889–7895, 2015.
- Yang, Z. and Khalighi, B.: CFD simulations for flow over pickup trucks, Tech. rep., SAE Technical Paper, 2005.
- Yelland, M., Moat, B., Taylor, P., Pascal, R., Hutchings, J., and Cornell, V.: Wind stress measurements from the open ocean corrected for airflow distortion by the ship, *Journal of physical Oceanography*, 28, 1511–1526, 1998.
- 450 Zazzeri, G., Lowry, D., Fisher, R., France, J., Lanoisellé, M., and Nisbet, E.: Plume mapping and isotopic characterisation of anthropogenic methane sources, *Atmospheric Environment*, 110, 151–162, 2015.